Steps in gas-surface reactions

Lent, R. van

Chapter 3

Site-specific reactivity of molecules with surface defects – the case of H_2 dissociation on Pt

The classic system that describes weakly activated dissociation in heterogeneous catalysis has been explained by two dynamical models that are fundamentally at odds. Whereas one model for hydrogen dissociation on Pt(1 1 1) invokes a pre-equilibrium and diffusion toward defects, the other is based on direct and localized dissociation. We resolve this dispute by quantifying site-specific reactivity using a curved Pt single crystal surface. Reactivity is step type dependent and varies linearly with step density. Only the model that relies on localized dissociation is consistent with our results. Our approach provides absolute, site-specific reaction cross sections.

Introduction

At the heart of any chemical transformation lie the dynamical events associated with elementary reactions. In gas phase reactions, reactant energy is redistributed over the limited degrees of freedom available in the products. For gas-surface collisions, the bulk provides a massive sink for energy dissipation. This makes mechanistic problems for gas-surface reactions quite challenging, as exemplified by ongoing discussion regarding the role of phonons and electron-hole pairs in surface reactions.[57, 58] In addition, surface heterogeneity may cause site-specific reactions to dominate overall kinetics in catalysis. For example, CO oxidation was recently shown to be site-specific on both Pt[47] and Pd[45].

The prototypical system in heterogeneous catalysis is H_2 dissociation on Pt. It is essential to the development of chemically accurate theoretical modeling of gas-surface interactions.[59] It is clear that H_2 dissociation occurs through dynamical processes.[59, 60] However, after four decades of research, two opposing dynamical models describing H_2 dissociation prevail in the literature. The fundamental discrepancy between the models lies in the assumed fate of kinetic energy of incident molecules. In the first model, it is conserved in the collision and incident molecules elastically scatter into a precursor state. In the second model, incident kinetic energy is not conserved. Depending on the exact point of impact, it couples directly to the dissociation coordinate or is dissipated, for example, by excitation of a frustrated rotation.

The two models for H_2 dissociation on Pt surfaces are illustrated in figure 3.1. Model 1, schematically shown in figure 3.1a, was proposed by Poelsema, Lenz, and Comsa.[61, 62] Scattering experiments have previously shown that atoms and molecules may diffract into a physisorbed state.[63, 64] In their model, the elastic collision only leads to dissociation when a H_2 molecule also encounters a defect during friction-free diffusion across the

surface. The model is summarized by:

$$H_2(g) \underset{k_{des}}{\overset{k_{ads}}{\rightleftharpoons}} H_{2,phys} \xrightarrow{k_{defect}} 2H_{ads} \tag{3.1}$$

The rate constant for adsorption (k_{ads}) depends on the probability to resonantly scatter into the physisorbed state ($S_{0,nL}$). The rates at which physisorbed molecules desorb (k_{des}) or encounter defects (k_{defect}) depend on their velocity (ν), residence time (τ), and the average distance between defects (L_d). The model predicts a dissociation probability on the clean surface, S_0:

$$S_0 \propto S_{0,nL}\left(1 - e^{-\frac{L_d}{\nu\tau}}\right) \tag{3.2}$$

For large distances between defects, reactivity is rather sensitive to L_d. For short distances, i.e. higher defect densities, this sensitivity is lost. The transition occurs when the physisorbed molecule has a mean free path, i.e. $\nu \cdot \tau$, comparable to the distance between defects.

In model 2, Baerends and coworkers,[65] Hayden and coworkers,[66] and Somorjai and coworkers[67] propose parallel dynamical mechanisms for different surface sites, e.g. terraces and steps. None of these mechanisms contains a long-lived, diffusing precursor state. Dissociation is adequately represented as elementary:

$$H_2(g) \quad \xrightarrow{k_{ave}} \quad 2H_{ads} \tag{3.3}$$

The observed reactivity represents an average (k_{ave}) from site-specific contributions. Terraces contribute by direct dissociation, as illustrated in figure 3.1b. Incident kinetic energy is used to surmount activation barriers that vary with exact location and molecular orientation. Steps contribute by the two mechanisms illustrated in figures 3.1c and 3.1d. The first occurs at the cusp and is responsible for the initial negative correlation of reactivity with incident kinetic energy (E_{kin}).[66, 68] Dynamical calculations suggest that kinetic energy is converted to molecular rotation. Dissociation occurs when the dynamically trapped molecule senses the upper edge of the step.[65] The second contribution by steps is barrier-free dissociation at the upper edge.[65, 66, 68–70] Kinetic energy flows into the reaction coordinate

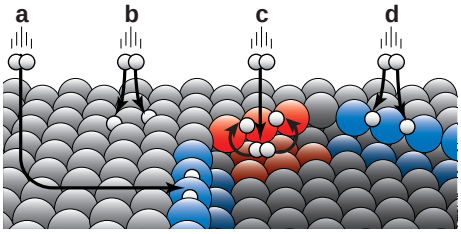

Figure 3.1: a) Model 1: mobile precursor mechanism. b) Model 2: direct activated dissociation at (1 1 1) terraces. c) Model 2: trapping mediated dissociation at step edges. d) Model 2: direct dissociation at step edges. A- and B-type steps are shown in blue and red respectively. c) and d) can take place at either step type but relative contributions may vary.

and is quickly lost to the substrate. The reactivity constant in this model can be represented as the weighted average of site-specific reactivities, S_0^{site},

$$S_0 \propto \sum_{site} f^{site} \cdot S_0^{site} \tag{3.4}$$

In contrast to the previous one, this second model thus predicts a strictly linear relation between reactivity and the fractional occurance of each type of reactive site, f^{site}. Whereas the first model also did not discriminate between defects, this model does allow for varying contributions by, e.g., the A- and B-type step edges depicted in figure 3.1.

A new approach allows us to test both models on a single sample. The step density along a curved Pt surface has been shown to vary smoothly from 'defect free' (1 1 1) to highly stepped surfaces.[36] By combining a curved surface approach and supersonic molecular beam methods [30] with highly improved spatial resolution, we resolve that H_2 dissociation does not require physisorption and diffusion to defect sites. In addition, we quantify site-specific reactivities for both {0 0 1} (A-type) and {1 1 0} (B-type) step types.

Method

A schematic illustration of the experiment is shown in figure 3.2a-e. Our Pt single crystal is cut as a 31° section of a cylinder along the [1 $\bar{1}$ 0]

rotational axis. The (1 1 1) surface appears at the apex.[71] The macroscopic curvature of the crystal is a direct result of monatomic steps.[36] Consequently, the local surface structure on our crystal varies smoothly from Pt(3 3 5) via Pt(1 1 1) to Pt(5 5 3).[71] As both A- and B-type steps are spatially separated by the (1 1 1) surface, their influence on reactivity can be probed independently. We measure initial sticking probabilities (S_0) using the King and Wells approach (see chapter 2).[11] The molecular beam is incident on the surface along the [1 1 1] vector. We measure S_0 as a function of step density by translating the single crystal surface with respect to our rectangular-shaped supersonic molecular beam (0.126 x 6.0 mm^2). Figure 3.2d illustrates the relative sizes of the crystal and the beam. Figure 3.2e quantifies the convolution of the narrow molecular beam with step density. Near (1 1 1) it is limited to 0.01 nm^{-1}. Our measurements are limited to step densities of 0.8 nm^{-1} due to narrowing of the crystal at high step densities in combination with the 6 mm width of our beam.

Results and Discussion

Figure 3.2f shows S_0 at a surface temperature (T_s) of 155 K as a function of step density and step type for E_{kin} = 9.3 meV and 100 meV. These energies are produced by (anti)seeding D_2 beams and estimated from time of flight measurements. At the lower E_{kin}, S_0 starts at 0.01±0.05 for the (1 1 1) surface and increases linearly with step density. S_0 for B-type step edges are consistently higher than A-type step edges at similar step density. At the higher E_{kin}, the influence of steps has disappeared and S_0 is approximately constant over the entire step density range. This energy dependence is consistent with all previous King and Wells studies of H_2 dissociation on flat and stepped single crystal surfaces. [18, 66, 68–70, 72]

For the lower E_{kin}, where steps are the dominant source of dissociation, figure 3.3 compares S_0 as a function of step density for T_s = 155 K and 300 K. Results are only shown for B-type steps, but the trend is identical for A-type steps. Also shown as dashed lines are predictions for S_0 by model 1,[62] as described in appendix B. The curvature in the predicted step density

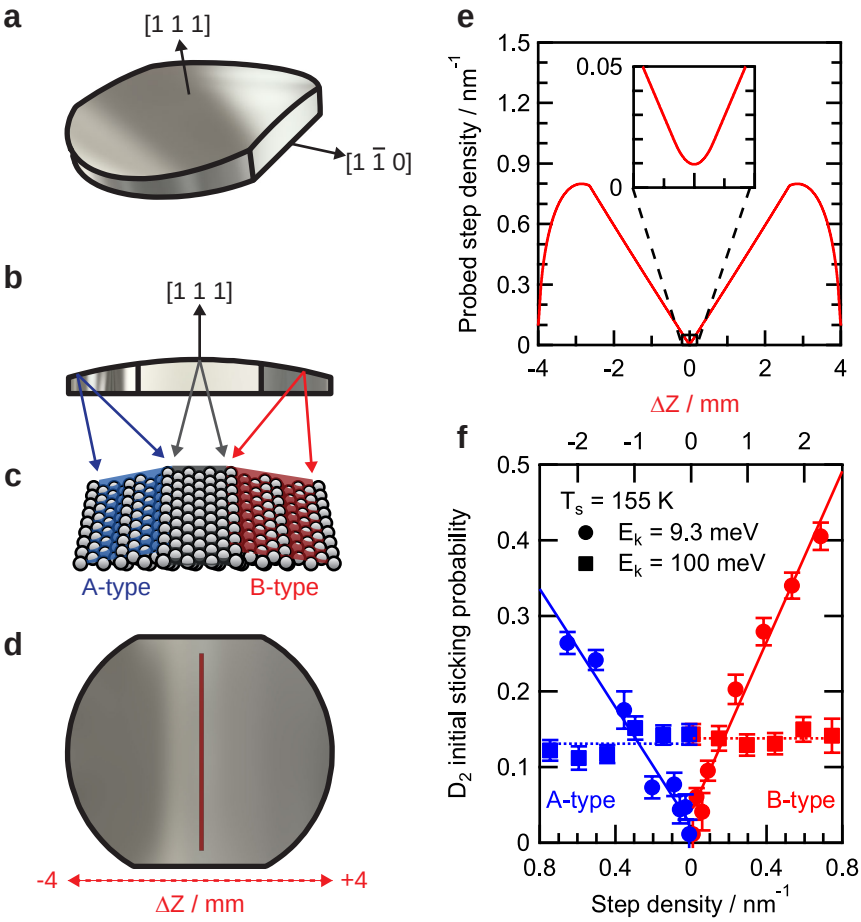

Figure 3.2: a) Birdseye view of the curved Pt single crystal. b) Side view along the [1 1̄ 0] vector. c) Side view showing the surface structure and surface planes of Pt(3 3 5) (A-type steps), Pt(1 1 1), and Pt(5 5 3) (B-type steps) in blue, gray, and red, respectively. d) Top view with the molecular beam size in red. e) Step density probed by the molecular beam at the position relative to the (1 1 1) surface. f) S_0 (D_2) at T_s = 155 K as a function of step density. Results from A- and B-type step edges are depicted in blue and red. Circles and squares represent E_{kin} = 9.3 meV and E_{kin} = 100 meV. Lines are least square fits to the data. Error bars represent the standard deviation in S_0.

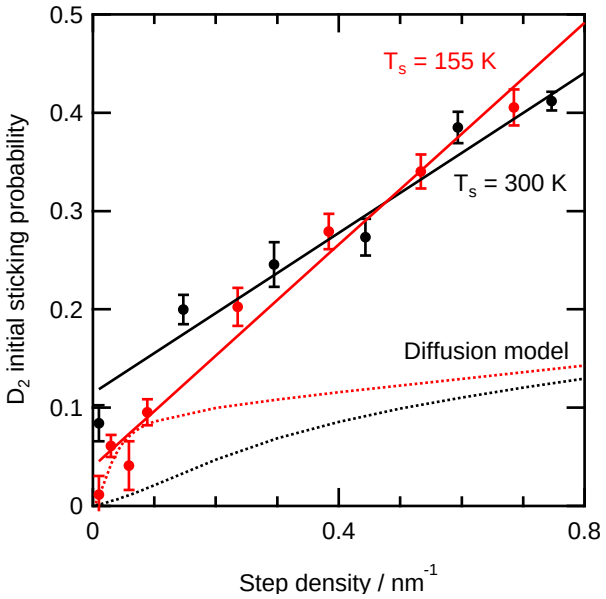

Figure 3.3: S_0 (D_2) for E_{kin} = 9.3 meV as a function of B-type step density. Circles are measured data. Solid lines are fits to the data. Dashed lines are predicted results from model 1. Red and black represent T_s = 155 K and 300 K respectively. Error bars represent the standard deviation in S_0.

dependence is a logical consequence of model 1. When the 'mean free path' of the physisorbed state approaches or exceeds the distance between defects, increasing defect density becomes less effective in increasing S_0. Only at high defect density, does S_0 become proportional to step density.

Our results are clearly at odds with the predictions by this model. Not only is S_0 underestimated over the entire defect density range, two crucial dependencies are not reproduced in the experiment. First, predicted curvature in the S_0 dependence on step density near the (1 1 1) surface is absent. Second, the T_s dependence opposes the predicted trend. Whereas model 1 clearly reduces S_0 with increasing T_s due to the diminishing residence time in a physisorbed state, we find that S_0 generally increases or is hardly affected. An attempt to improve the model by incorporating Debye-Waller

attenuation, reducing the probability of scattering into the resonant state, would increase this discrepancy. In addition to these erroneous dependencies, the site-specific reactivity of S_0 seen in figure 3.2f is not captured in model 1. Finally, it also does not capture the observed step density independence at the higher E_{kin}.

In contrast, our results are in agreement with the two underlying assumptions of model 2. Terrace and step sites contributing proportionally to their abundance and the absence of a freely diffusing precursor require a strictly linear dependence of S_0 on step density. Least squares fitting yields a residual reactivity due to dissociation on the Pt(1 1 1) surface. Individual fits to A- and B-type steps for lower incident energy yields 0.023±0.009 and 0.040±0.008. This is in good agreement with previous results[18, 72] for Pt(1 1 1), even with experimental results for the clean 'defect free' surface [61] on which model 1 is based. This residual reactivity of the 'defect free' Pt(1 1 1) surface is explained by recent dynamical calculations for D_2 dissociation.[73] Select impact geometries show barrier-free dissociation on the Pt(1 1 1) surface.

The slope of the linear fits in figure 3.2f reflect the summed contributions of direct barrier-free and trapping-mediated dissociation at step edges, shown in figures 3.1c-d. Multiplying the slope of each linear fit with the width of the unit cell yields the reaction cross section for H_2 dissociation at the step edge.[70] For our low E_{kin} data at T_s = 155 K, these are 0.108±0.007 and 0.157±0.007 nm^2 for A- and B-type steps. The reaction cross section for A-type steps agrees quantitatively with theoretical results that show the surface area of the Pt(1 1 2) unit cell where impact at the step results in dissociation.[65] We previously showed that the direct contribution at the upper edge, shown in figure 3.1d, amounts to 0.043 nm^2.[70] The trapping-mediated mechanism in figure 3.1c is then responsible for the 0.065 nm^2 difference at A-type steps. As the local structure at the upper edge is identical, the significantly larger cross section for B-type steps compared to A-type steps suggests larger and/or deeper molecular chemisorption wells at its cusp.

Conclusion

In summary, the model ascribing H_2 dissociation on Pt mostly to a highly mobile precursor fails to predict the reactivity dependence on step density and surface temperature. In addition to a lack of site specificity, the model erroneously assumes that the perfect Pt(1 1 1) surface only exhibits activated adsorption.[73] As reactivity in this model is fully ascribed to defects, the model's parameters and other conjectures must reflect this overestimate. We believe this to be represented by the unphysical assumption that all scattering occurs into the ground vibrational level of the physisorbed state. Furthermore, while the model's parameters are based on a fit to experimental data using dissociation from a bulb gas at room temperature, the known complex angular dependence to dissociation [18, 74] is not taken into account. More assumptions may contribute to its failure, e.g. that no other possible outcome than dissociation exists when physisorbed molecules encounter a defect.

Simultaneously, our data support that dissociation is dominated by impulsive interactions at the impact site. In the relevant regime, there is no significant surface temperature dependence and, at low kinetic energy, dissociation is strictly linear with step density. At incident energies exceeding most barriers to dissociation on the terrace, the contribution of steps becomes indiscernible; reactivity becomes independent of step density. From our low kinetic energy data, we extract site-specific reaction cross sections for A- and B-type step edges in a chemical reaction. The reaction cross section of B-type steps is significantly larger than that of A-type steps, suggesting a larger molecular chemisorption well with more efficient kinetic energy dissipation. These results present benchmarks for future construction of high dimensional potential energy surfaces and guide dynamical studies aiming to understand the kinetics of this prototypical system. In particular, the origin of the significantly larger cross section for dissociation at B-type step edges may be extracted from calculation of the potential energy surface of H_2/Pt(2 2 1). Additional (quantum) dynamical calculations, similar to those performed by Baerends and coworkers[65, 75]

could confirm the dominant contributions of the three parallel dynamical mechanisms captured by model 2.